

A Nonlinear Subgrid Stabilization Parameter-Free Method to Solve Incompressible Navier-Stokes Equations at High Reynolds Numbers

Riedson Baptista[1,2(✉)], Sérgio S. Bento[2(✉)], Leonardo M. Lima[3], Isaac P. Santos[1,2(✉)], Andrea M. P. Valli[1], and Lucia Catabriga[1]

[1] High Performance Computing Lab, Federal University of Espírito Santo, Vitória, ES, Brazil
{riedson.baptista,isaac.santos}@ufes.br, {avalli,luciac}@inf.ufes.br

[2] Department of Applied Mathematics, Federal University of Espírito Santo, São Mateus, ES, Brazil
sergio.bento@ufes.br

[3] Department of Mechanical Engineering, Federal Institute of Espírito Santo, Aracruz, ES, Brazil
lmuniz@ifes.edu.br

Abstract. In this work we evaluate a Nonlinear Subgrid Stabilization parameter-free method to solve time-independent incompressible Navier-Stokes equations (NSGS-NS) at high Reynolds numbers, considering only the decomposition of the velocity field (not pressure) into coarse/resolved scales and fine/unresolved scales. In this formulation we use a dynamic damping factor which it is often essential for the nonlinear iterative process and for the reduction of the number of iterations. In order to reduce the computational costs typical of two-scale methods, the unresolved scale space is defined using bubble functions whose degrees of freedom are locally eliminated in favor of the degrees of freedom that live on the resolved scales. Accuracy comparisons with the streamline-upwind/Petrov-Galerkin (SUPG) formulation combined with the pressure stabilizing/Petrov-Galerkin (PSPG) are conducted based on 2D steady state benchmark problems with high Reynolds numbers, flow over a backward-facing step and lid-driven square cavity flow.

Keywords: Incompressible Navier-Stokes equation · Nonlinear Subgrid Stabilization · Variational multiscale method · Damping factor

1 Introduction

The Navier-Stokes equations are at the heart of fluid flow modeling, where many phenomena of scientific and engineering interest are modeled by them.

© Springer Nature Switzerland AG 2019
S. Misra et al. (Eds.): ICCSA 2019, LNCS 11621, pp. 134–148, 2019.
https://doi.org/10.1007/978-3-030-24302-9_11

The momentum and continuity equations, with velocity field and pressure as the unknowns, compose the Navier-Stokes equations. Regardless of the chosen discretization method, solving the Navier-Stokes causes many numerical and computational problems. In general, the numerical methods involve a significant time of calculations. Moreover, problems arise when the finite element method is used to solve the Navier-Stokes equations related, for example, if the velocity and pressure spaces do not fulfill the Ladyzhenskaya-Babuska-Brezzi (LBB) condition [6]. Another source of numerical difficulty is the presence of the nonlinear convective term. Because of that, most finite element techniques and computations reported in the past three decades are based on stabilized formulations. Furthermore, high Reynolds number flows are convection dominated and stabilization techniques with special nonlinear treatment must be used to avoid non-physical oscillation.

Many stabilized finite element formulations have been used to solve the Navier-Stokes equations. The streamline-upwind/Petrov-Galerkin (SUPG) [8] formulation combined with the pressure stabilizing/Petrov-Galerkin (PSPG) [24] was the precursor of the Galerkin/Least-Squares (GLS) stabilization methods [23], or its modification proposed in [15]. Another class of stabilized methods based on the idea of augmenting the Galerkin method with virtual bubble functions was introduced in [7]. All approaches try to reduce the numerical instabilities present at problems with high Reynolds or Mach numbers, shocks or thin boundary layers, and equal-order interpolation functions for velocity and pressure.

The variational multiscale (VMS) methodology was introduced by Hughes in [22] for the scalar convection-diffusion equation and extended for the Navier-Stokes equations by a set of researchers [4,10,11,19,27]. Recently, we present a nonlinear multiscale parameter-free method (NSGS-NS) to solve incompressible flow problems [3], consisting of a decomposition for both velocity and pressure fields into coarse/resolved and fine/unresolved scales, together with the addition of a residual-based nonlinear operator to the enriched Galerkin formulation. In this approach, the pressure fine-scale is approximated using a heuristic scaling of the continuity equation [9], based on the incompressibility constraint (LSIC) parameter [26]. We observed that the pressure solution did not present satisfactory results for the experiments performed there.

In this paper, we consider only the decomposition of the velocity field into resolved and unresolved scales, as it is considered in [19] – the pressure unknowns live onto the resolved scale. Since the subgrid scales are modeled by bubble functions, this approach leads to a numerical formulation satisfying the LBB condition, that can be considered an extension of the MINI element [2] to the Navier-Stokes equations. Besides of that, the artificial nonlinear viscosity operator described in [3] is added to the unresolved scales in order to stabilize the velocity field at high Reynolds number. Generally, the nonlinearity became more representative when the Reynolds numbers increase, needing a dynamic damping process to improve the convergence. Here, we use the dynamic dam-ping algorithm proposed in [25].

The remainder of this work is organized as follows. Section 2 briefly addresses the governing equations and the variational multiscale formulation. In the next section, we show the numerical formulation with the dynamic damping factor algorithm. Section 4 evaluates the numerical performance of two 2D benchmark problems for incompressible flow problems at high Reynolds numbers, and Sect. 5 concludes the paper.

2 The Incompressible Navier Stokes Equations

The incompressible Navier-Stokes equations result from the conservation principles of momentum and mass. Using primitive variables, the stationary case of these equations in two dimensions read

$$(\boldsymbol{u}\cdot\nabla)\boldsymbol{u} - 2\nu\nabla\cdot\boldsymbol{\varepsilon}(\boldsymbol{u}) + \nabla p = \boldsymbol{f},\ \text{in } \Omega, \tag{1}$$

$$\nabla\cdot\boldsymbol{u} = 0,\ \text{in } \Omega, \tag{2}$$

where $\boldsymbol{u} = (u, v)$ is the velocity field, p is the kinematic pressure, ν is the kinematic viscosity, $\boldsymbol{f}$ is a body force, and $\boldsymbol{\varepsilon}(\boldsymbol{u})$ is the strain rate tensor defined as

$$\boldsymbol{\varepsilon}(\boldsymbol{u}) = \frac{1}{2}(\nabla\boldsymbol{u} + (\nabla\boldsymbol{u})^T).$$

These equations have to be solved in the domain $\Omega \subset \mathbb{R}^2$ with a smooth boundary Γ. Moreover, to provide a well-posed mathematical problem, a set of appropriate boundary conditions is added to equations system (1)–(2).

2.1 The Variational Formulation

The Galerkin finite element discretization of the Navier-Stokes equations (1)–(2) is based on its variational formulation. For simplicity, considering homogeneous Dirichlet boundary conditions for the velocity field, the variational formulation consists of finding $\boldsymbol{u} \in V$ and $p \in Q$ such that

$$\int_\Omega \boldsymbol{w}\cdot(\boldsymbol{u}\cdot\nabla\boldsymbol{u})\ d\Omega + 2\nu\int_\Omega \boldsymbol{\varepsilon}(\boldsymbol{w}):\boldsymbol{\varepsilon}(\boldsymbol{u})\ d\Omega - \int_\Omega p\nabla\cdot\boldsymbol{w}\ d\Omega = \int_\Omega \boldsymbol{w}\cdot\boldsymbol{f}\ d\Omega;$$

$$\int_\Omega q\nabla\cdot\boldsymbol{u}\ d\Omega = 0,$$

for all $\boldsymbol{w} \in V$ and $q \in Q$, where

$$V = [H_0^1(\Omega)]^2, \quad Q = L_0^2(\Omega) = \left\{p \in L^2(\Omega);\quad \int_\Omega p\ d\Omega = 0\right\}. \tag{3}$$

It is well known that the standard Galerkin finite element method is not suitable for solving the incompressible Navier-Stokes equations. The user has to choose functions spaces for velocity and pressure that satisfy the LBB condition

[6], for example, the Taylor-Hood and MINI elements [2,5,21]. Moreover, due to the presence of the nonlinear convective term, in the convection dominated regime (flows at high Reynolds number), stabilization techniques with special nonlinear treatment are required to provide stable numerical solutions. In the next section we present the Nonlinear Subgrid Stabilization method, presented in [3], for solving the problem (1)–(2).

3 The Numerical Formulation

The numerical formulation is constructed projecting the problem onto the finite-dimensional subspaces $V_h \subset V$ and $Q_h \subset Q$. To define the subspaces V_h and Q_h, we consider a triangular partition $\mathcal{T}_h$ of the domain Ω into n_{el} elements, where $\Omega = \bigcup_{e=1}^{n_{el}} \Omega_e$ and $\Omega_i \cap \Omega_j = \emptyset$, $i, j = 1, 2, \cdots, n_{el}$, $i \neq j$. Thus, the finite element subspaces V_h and Q_h are given by

$$V_h = \{\boldsymbol{u}_h \in [H_0^1(\Omega)]^2; \boldsymbol{u}_h|_{\Omega_e} \in [\mathbb{P}_1(\Omega_e)]^2\};$$
$$Q_h = \{p_h \in H^1(\Omega); p_h|_{\Omega_e} \in \mathbb{P}_1(\Omega_e), \int_\Omega p_h \, d\Omega = 0\},$$

where $\mathbb{P}_1(\Omega_e)$ is the set of first order polynomials in Ω_e. Consider the enriched space

$$V_h^b = V_h \oplus V_b,$$

given by the direct sum of V_h, the standard finite element space, and of V_b, a space spanned by bubble functions (a polynomial function ψ_b which takes the value 1 at the barycenter of the element Ω_e, vanishes on its boundary $\partial\Omega_e$ and satisfies $0 \leq \psi_b \leq 1$), described as

$$V_b = \{\boldsymbol{u}_b \in [H_0^1(\Omega)]^2; \boldsymbol{u}_b|_{\Omega_e} \in [span(\psi_b)]^2, \forall \Omega_e \in \mathcal{T}_h\}.$$

The space V_h is called resolved scale space, whereas V_b is known as unresolved scale space. Solving the incompressible Navier-Stokes equation on spaces V_h^b for velocity and Q_h for pressure leads to a numerical formulation that can be considered an extension of the MINI element [2], a pair of elements satisfying the LBB condition, to the Navier-Stokes equations.

The Nonlinear Subgrid Stabilization (NSGS-NS) method for solving the incompressible Navier-Stokes equations consists of finding $\boldsymbol{u}_h^b = \boldsymbol{u}_h + \boldsymbol{u}_b \in V_h^b$ and $p_h \in Q_h$, with $\boldsymbol{u}_h \in V_h$ and $\boldsymbol{u}_b \in V_b$, such that

$$\int_\Omega \boldsymbol{w}_h^b \cdot (\boldsymbol{u}_h^b \cdot \nabla \boldsymbol{u}_h^b) \, d\Omega + 2\nu \int_\Omega \boldsymbol{\varepsilon}(\boldsymbol{w}_h^b) : \boldsymbol{\varepsilon}(\boldsymbol{u}_h^b) \, d\Omega \tag{4}$$

$$- \int_\Omega p_h \nabla \cdot \boldsymbol{w}_h^b \, d\Omega + \sum_{e=1}^{nel} \int_{\Omega_e} \nabla \boldsymbol{w}_b : (\delta_b \nabla \boldsymbol{u}_b) \, d\Omega = \int_\Omega \boldsymbol{w}_h^b \cdot \boldsymbol{f} \, d\Omega; \tag{5}$$

$$\int_\Omega q_h \nabla \cdot \boldsymbol{u}_h^b \, d\Omega = 0, \tag{6}$$

for all $\boldsymbol{w}_h^b \in V_h^b$ and $q_h \in Q_h$, with $\boldsymbol{w}_h \in V_h$ and $\boldsymbol{w}_b \in V_b$. To the Galerkin formulation is added the artificial nonlinear viscosity operator

$$\sum_{e=1}^{nel} \int_{\Omega_e} \nabla \boldsymbol{w}_b \colon (\delta_b \nabla \boldsymbol{u}_b)\, d\Omega,$$

acting only on the unresolved scales. The amount of artificial viscosity δ_b is calculated on the element-level according to

$$\delta_b = \delta_b(\boldsymbol{u}_h, p_h) = \begin{cases} \dfrac{h}{2} \dfrac{\|R(\boldsymbol{u}_h, p_h)\|}{\|\nabla(\boldsymbol{u}_h, p_h)\|}, & \text{if } \|\nabla(\boldsymbol{u}_h, p_h)\| > 0; \\ 0, & \text{otherwise,} \end{cases} \tag{7}$$

where $\|\cdot\|$ denotes the Euclidean norm and

$$R(\boldsymbol{u}_h, p_h) = \begin{cases} (\boldsymbol{u}_h \cdot \nabla)\boldsymbol{u}_h - 2\nu\nabla \cdot \boldsymbol{\varepsilon}(\boldsymbol{u}_h) + \nabla p_h - \boldsymbol{f} \\ \nabla \cdot \boldsymbol{u}_h \end{cases}$$

is the residue of the problem associated to the resolved scales on Ω_e. The details of the construction of the matrices associated with the problem and the static condensation process are described in [3].

The linearization process of the resulting system – for example, by fixed point or Newton methods – aims to generate a monotonous decreasing sequence of residues. However, most nonlinear stabilization methods can present difficulties in the convergence process of the nonlinear iterations. There are some naivy strategies described in the literature to improve the convergence of these methods [28,30]. Besides that, for more complex problems with large numbers of Reynolds, some nonlinear iterations may result in solutions that produce an increasing sequence of these residues, resulting in the divergence of the iterative process. Since we can not rule out such a solution and use it completely makes the process inefficient, we use only a small percentage of this solution. Thus we introduce a damping factor in the nonlinear iterative process, reducing the influence of such bad solutions. This damping factor can be a given value or generated dynamically. In our experiments, when the convergence of the nonlinear iterative method is not achieved, we use an adaptive process to choose this damping factor presented in [25] given by Algorithm 1.

We consider the damping factor $\omega \in [\omega_{min}, \omega_{max}]$, where $\omega_{min} = 0.05$ and $\omega_{max} = 1.0$. The actual solution $\boldsymbol{U}_h^{k+1}$ is calculated in line 9 of the Algorithm. It is accepted if $\|R(\boldsymbol{U}_h^{k+1})\| < \|R(\boldsymbol{U}_h^k)\|$ or if the factor ω has reached the lower limit. If $\|R(\boldsymbol{U}_h^{k+1})\| < \|R(\boldsymbol{U}_h^k)\|$ and ω has not reached its maximum value, it is incremented and iterative process goes on. When $\|R(\boldsymbol{U}_h^{k+1})\| > \|R(\boldsymbol{U}_h^k)\|$, the solution $\boldsymbol{U}_h^{k+1}$ is rejected and ω has its value reduced. In this case, a new value for $\boldsymbol{U}_h^{k+1}$ is calculated and the residue is evaluated again.

Algorithm 1. Dynamic choice of the damping factor

$\omega_{min} := 0.05$; $\omega_{max} := 1.0$;
$c_1 := 1.001$; $c_2 := 1.1$; $c_3 := 1.001$; $c_4 := 0.9$;
initialize $\boldsymbol{U}_h^0 = \mathbf{0}$ and compute residual $\|R(\boldsymbol{U}_h^0)\|$;
$\omega := \omega_{max}$; $k := 0$; $switch := 1$;
while $\|R(\boldsymbol{U}_h^k)\| > tolerance$ **do**
    compute $\Delta \boldsymbol{U}_h^{k+1}$;
    first-damping := 1;
    while $switch = 1$ **do**
        $\boldsymbol{U}_h^{k+1} := \boldsymbol{U}_h^k + \omega \Delta \boldsymbol{U}_h^{k+1}$;
        compute residual $||R(\boldsymbol{U}_h^{k+1})||$;
        if $\|R(\boldsymbol{U}_h^{k+1})\| < \|R(\boldsymbol{U}_h^k)\|$ **or** $\omega \leq c_1 \omega_{min}$ **then**
            if $\|R(\boldsymbol{U}_h^{k+1})\| < \|R(\boldsymbol{U}_h^k)\|$ **and** *first-damping* $= 1$ **then**
                $\omega_{max} := min\{1, c_3 \omega_{max}\}$;
                $\omega := min\{\omega_{max}, c_2 \omega\}$;
            end if
            $switch := 0$;
        else
            $\omega := max\{\omega_{min}, \omega/2\}$
            if *first-damping = 1* **then**
                $\omega_{max} := max\{\omega_{min}, \omega_{max}\}$;
                first-damping := 0;
            end if
        end if
    end while
    $k := k + 1$;
end while

4 Numerical Experiments

In the experiments, we consider two well-known 2D benchmark problems for incompressible flows with high Reynolds numbers: the "backward-facing step" and the "lid-driven cavity". Our multiscale methodology is compared to the SUPG/PSPG presented in [12,29]. We evaluate the numerical solutions obtained by both methods with the results presented in [13] for the "backward-facing step" problem and with the high accuracy experiments presented in [14,20] for the "lid-driven cavity" problem.

The nonlinear system generated by the methods of this work is solved by the Picard iterative process with $tol_{nl} = 10^{-3}$ and maximum number of nonlinear steps equal to $itmax_{nl} = 10^3$. The resulting linear systems are solved by GMRES

method with 45 vectors to restart, tolerance equals 10^{-12} with incomplete factorization ILU(10) preconditioners. The domains are discretized considering meshes generated by the Gmsh software [18] and the tests were performed on a machine with an Intel Core i5-6200U 2.3GHz×4 processor with 8GB of RAM and Ubuntu 18.04 operating system.

4.1 Flow over Backward-Facing Step

The backward-facing step problem is one of the most used and benchmarked geometry for computation fluid dynamic and experimental flow analysis. It consists of a fluid flowing into a straight channel which abruptly widens on one side, see Fig. 1(a) for the problem description. It produces a recirculation zone on the lower channel wall and a recirculation zone farther downstream on the upper wall, with high Reynolds numbers [1,13,17]. Here, the inlet velocity field is specified as a parallel flow with a parabolic horizontal component given by $u(y) = -32/3y^2 + 24y - 12$ for $0,75 \leq y \leq 1.5$, which produces a maximum inflow velocity of $u_{max} = 1.5$ and an average inflow velocity of $u_{avg} = 1.0$.

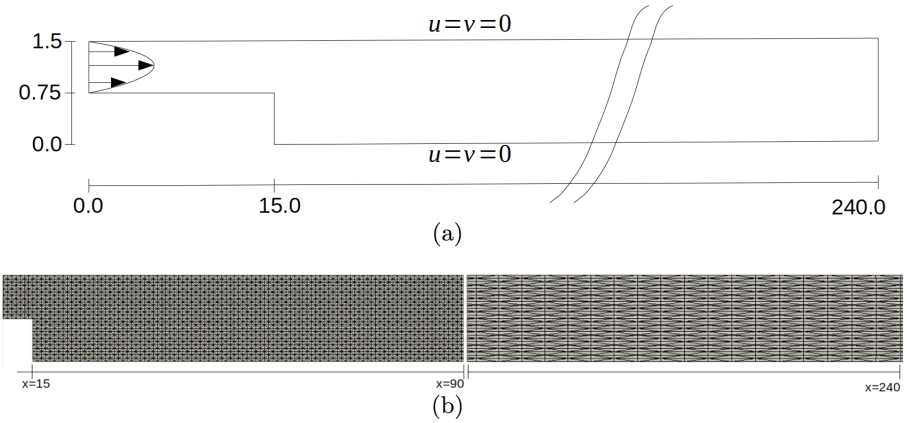


Fig. 1. Flow over a backward facing step: (a) problem description and (b) finite element mesh (43259 nodes and 83070 elements).

Figure 1(b) shows the triangular mesh used in all experiments, with a deeper refinement before $x = 90$. The total number of nodes and elements are 43259 and 83070, respectively. The stream function contours in Fig. 2 illustrate the main features of the separated flows with $Re = 500, Re = 800$ and $Re = 1000$. Our results show excellent agreement with the high accuracy experiments presented in [1,13]. In Fig. 3, we show the horizontal velocity profiles at $x = 25.5$ and 37.5 streamwise locations, and we compare them with the experiments in [13]. Our NSGS-NS solutions show very good agreement with them, at both $x = 25.5$ and 37.5 locations.

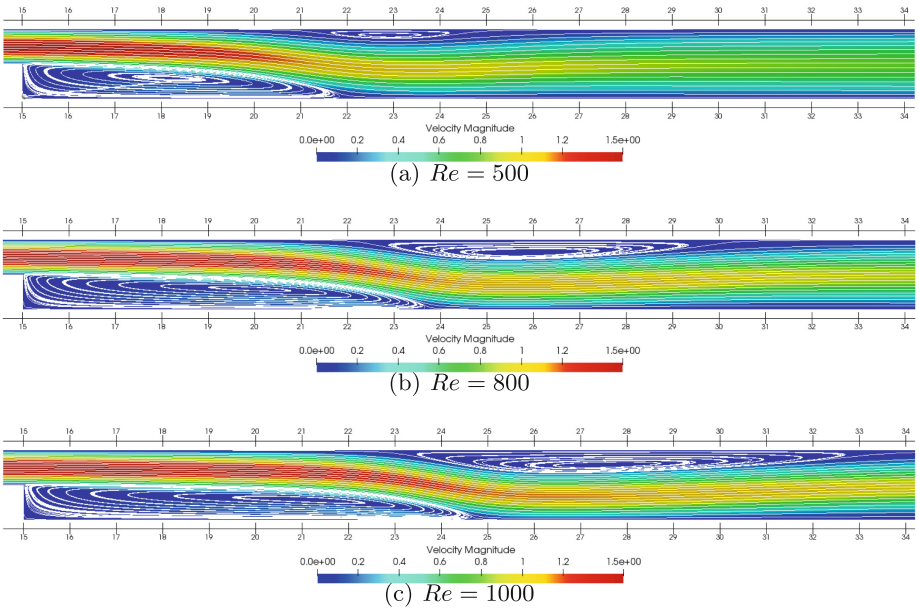


Fig. 2. Flow over a backward facing step: NSGS-NS solution with $Re = 500, 800, 1000$.

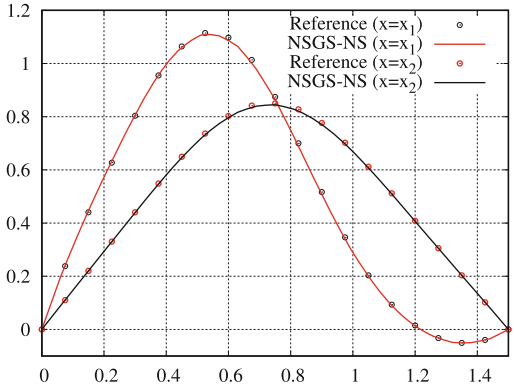


Fig. 3. Horizontal velocity profile for $Re = 800$ at two downstream locations, $x_1 = 25.5$ and $x_2 = 37.5$, with $0 \leq y \leq 1.5$.

In Table 1, we have tabulated our numerical results and reference values [13] for the dimensionless characteristic lengths x_1, x_2 and x_3, see Fig. 4, frequently used to characterize the simulation results of this problem. Those lengths are normalized by the channel step height h. As we can see, they are in an excellent agreement with the reference values observed in the reference. Moreover, the NSGS-NS method presents better solution for the characteristic lengths than the ones obtained by the SUPG/PSPG method.

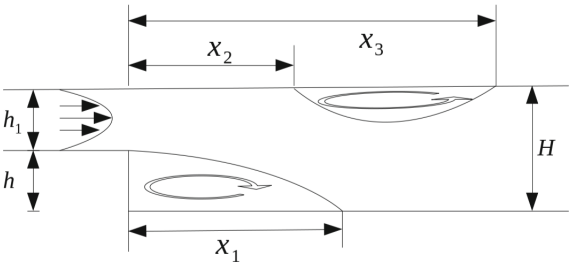


Fig. 4. Flow over a backward-facing step - characteristic lengths.

Table 1. Flow over a backward-facing step: characteristic lengths.

	$Re = 500$			$Re = 800$			$Re = 1000$		
	x_1/h	x_2/h	x_3/h	x_1/h	x_2/h	x_3/h	x_1/h	x_2/h	x_3/h
Reference [13]	9.42	8.013	13.171	11.834	9.476	20.553	13.121	10.474	24.882
NSGS-NS method	9.41	8.01	13.17	11.83	9.47	20.55	13.12	10.47	24.88
SUPG/PSGP method	9.33	8.27	12.93	11.47	9.07	19.87	12.67	10.07	24.07

Computational performance of both methods are shown in the Table 2, where $(\#NLI)$ is the number of nonlinear iterations, $(\#LI)$ is the number of GMRES iterations and $(Time)$ is the CPU time in seconds. Note that NSGS-NS number of nonlinear iterations is greater SUPG/PSPG iterations with all Reynolds numbers. However, the SUPG/PSPG nonlinear iterations consume more linear iterations and CPU time than the corresponding NSGS-NS solutions. Therefore, in addition to present better solutions, the NSGS-NS method is computationally more efficient.

Table 2. Flow over a backward-facing step: computational performance.

Methods	$Re = 500$			$Re = 800$			$Re = 1000$		
	$\#LI$	$\#NLI$	$Time(s)$	$\#LI$	$\#NLI$	$Time(s)$	$\#LI$	$\#NLI$	$Time(s)$
NSGS-NS	3972	52	245.32	6946	84	540.14	8719	101	734.31
SUPG/PSPG	22609	50	1247.06	47134	74	2257.29	63407	83	3271.85

4.2 The Lid-Driven Cavity Flow

The 2D lid-driven cavity flow problem has been widely used as a benchmark for numerical methods and has been analyzed by a number of authors [14,20]. The standard case is fluid contained in a square domain with Dirichlet boundary conditions on all sides, with three stationary sides and one moving side at the top, see Fig. 5. There are no body forces and the pressure is prescribed to be zero at the bottom left corner of the cavity. Here the domain is $\Omega = (0, 1)^2$ and

to avoid the irregularity of the solution at the upper corners [16], the horizontal velocity at the top side is given by

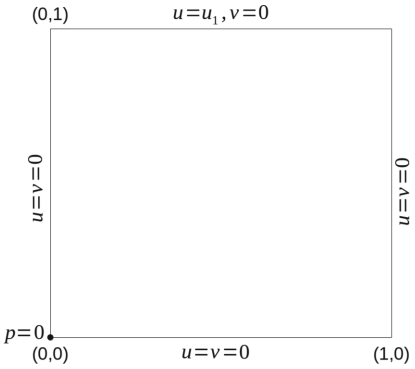
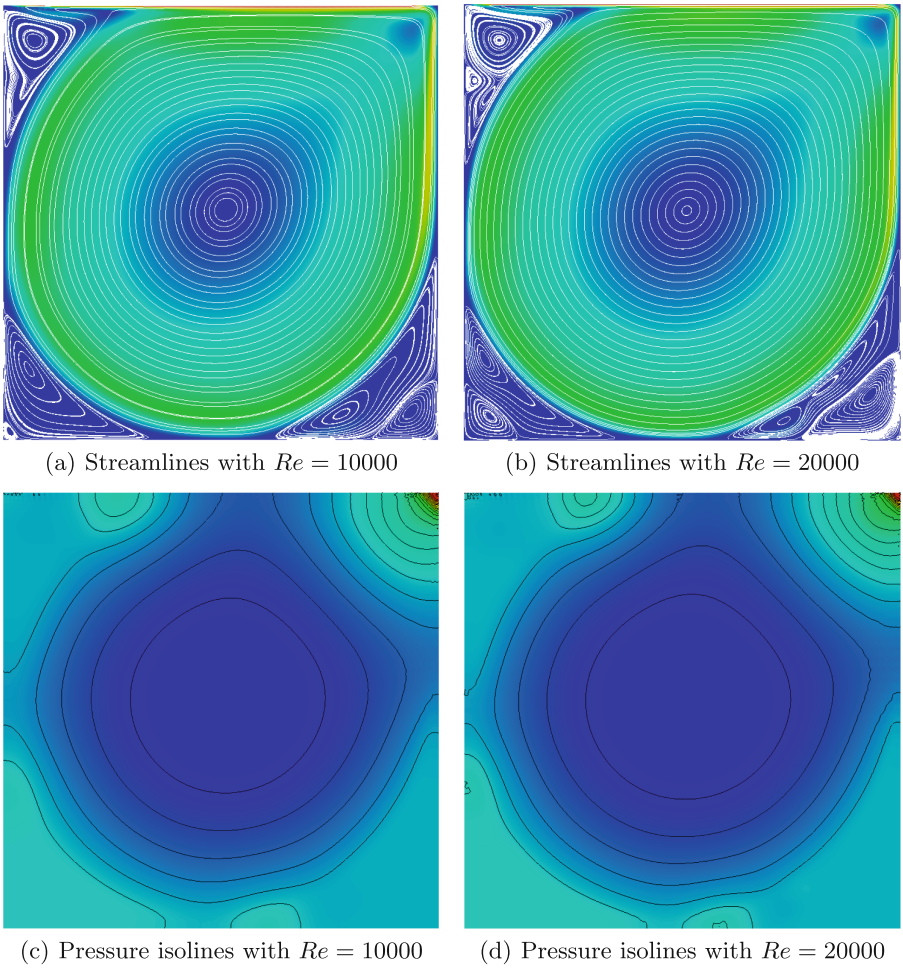


Fig. 5. The lid-driven cavity problem description.

$$u_1(x) = \begin{cases} 1 - \frac{1}{4}\Big(1 - \cos\big((0.1 - 1x)10\pi\big)\Big)^2 & \text{for } x \in [0, 0.1], \\ 1 & \text{for } x \in (0.1, 0.9), \\ 1 - \frac{1}{4}\Big(1 - \cos\big((x - 0.9)10\pi\big)\Big)^2 & \text{for } x \in [0.9, 1]. \end{cases}$$

As a result of the moving top side of the cavity, a recirculation region is developed that bears a primary vortex in the middle of the cavity and additional secondary vortices in the corners of the cavity. Figure 6 shows the streamlines and pressure isolines for the NSGS-NS method with $Re = 10000$ and $Re = 20000$, using a linear triangular finite element mesh with 14641 nodes. Our streamlines results show excellent agreement with the high accuracy experiments presented in [14,20]. For $Re = 10000$, our pressure isolines are comparable with the ones presented in [20]. In Fig. 7, we present the horizontal velocity along the vertical line $x = 0.5$ and the vertical velocity along the horizontal line $y = 0.5$. Comparing the NSGS-NS solutions with the given reference solutions in [14] (black points), one can clearly see perfect agreement between the solutions. We can also observe in Fig. 7 that the SUPG/PSPG solutions do not present good agreement with the reference solutions.

Table 3 shows the computational performance of NSGS-NS and SUPG/PSPG methods in terms of nonlinear iterations ($\#NLI$), GMRES iterations ($\#LI$) and CPU time in seconds ($Time$). As we can see, the NSGS-NS nonlinear iterative process does not converge without the damping factor process with both Reynolds numbers. In the SUPG/PSPG method, the dynamic choice is not necessary for convergence of the iterative processes, but the algorithm significantly reduces the CPU time improving the computational performance of the method.

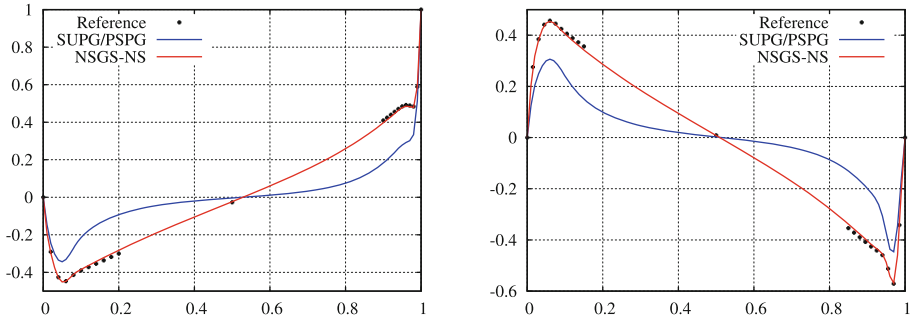


(a) Streamlines with $Re = 10000$ (b) Streamlines with $Re = 20000$

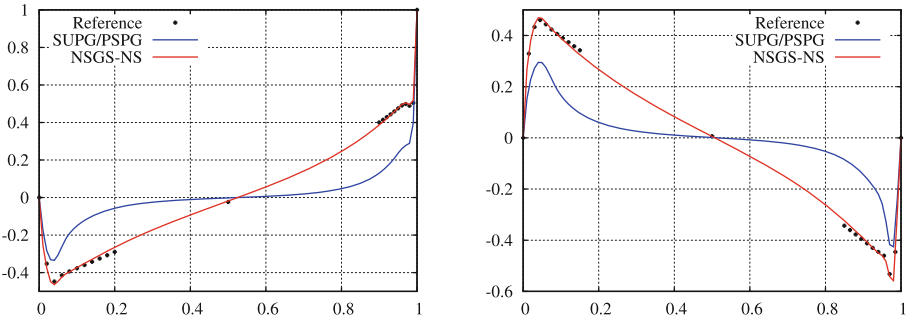
(c) Pressure isolines with $Re = 10000$ (d) Pressure isolines with $Re = 20000$

Fig. 6. The lid-driven cavity flow: streamlines and pressure isolines for the NSGS-NS method with $Re = 10000$ and $Re = 20000$.

Figure 8 shows the damping factor values required in each nonlinear iteration for both methods. In the SUPG/PSPG method, the damping factor increases in the course of the iterative process with only one rejection at the first iteration. Thus, the maximum possible number of iterations occurs in the beginning of the process improving the efficiency of the nonlinear iteration scheme. In the NSGS-NS method, there are some rejections but the dynamic process does not reduce the damping factor to the lower bound, $\omega_{min} = 0.05$. Observe also that, the strong damping necessary at the beginning of the iterative process slightly influences the damping at the end.



(a) $Re = 10000$.

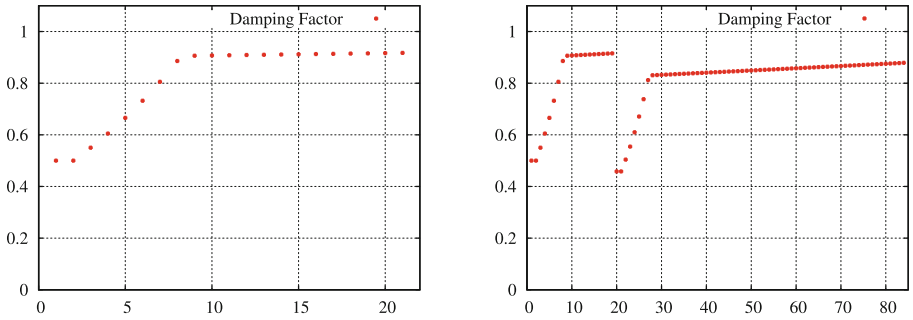


(b) $Re = 20000$.

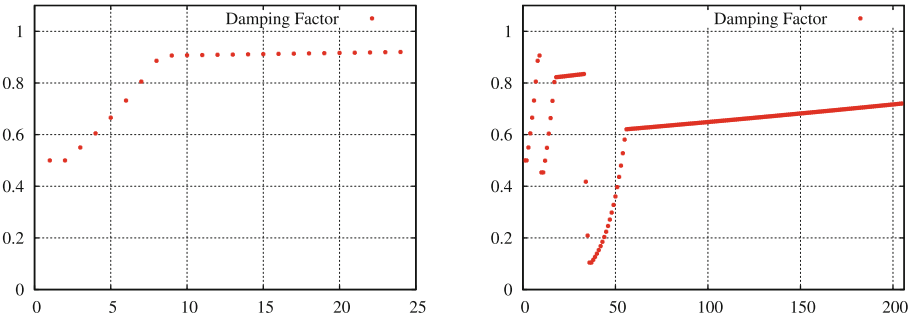
Fig. 7. The lid-driven cavity problem. Left: horizontal velocity along $x = 0.5, 0 \leq y \leq 1$, right: vertical velocity along $y = 0.5, 0 \leq x \leq 1$, (a) $Re = 10000$ and (b) $Re = 20000$.

Table 3. Performance computational. The lid-driven cavity flow.

Methods	$Re = 10000$			$Re = 20000$		
With damping factor	$\#LI$	$\#NLI$	$Time(s)$	$\#LI$	$\#NLI$	$Time(s)$
NSGS-NS	6300	84	150.13	14898	205	360.09
SUPG/PSPG	858	21	27.07	1020	24	35.76
Without damping factor	$\#LI$	$\#NLI$	$Time(s)$	$\#LI$	$\#NLI$	$Time(s)$
NSGS-NS	†	†	†	†	†	†
SUPG/PSPG	1316	32	41.63	1820	42	61.19



(a) $Re = 10000$.



(b) $Re = 20000$.

Fig. 8. The lid-driven cavity flow. Damping factor in each nonlinear iteration. Left: SUPG/PSPG method, right: NSGS-NS method, (a) $Re = 10000$ and (b) $Re = 20000$.

5 Conclusions

We evaluated the computational performance of the Nonlinear Subgrid Stabilization parameter-free method (NSGS-NS) [3] to solve the incompressible Navier-Stokes equations at high Reynolds numbers. The formulation considers a two-scale decomposition only of the velocity field, into coarse/resolved scales and fine/unresolved scales. Furthermore, we use a dynamic damping factor to improve the convergence of the nonlinear iterative process, in order to be able to solve flows at high Reynolds numbers.

With two 2D benchmark problems, we compare the proposed methodology with the SUPG/PSPG approach presented in [12,29]. In our studies, we investigate the backward facing step problem and the lid-driven cavity flow, at high Reynolds numbers. The solutions are compared with high accuracy experiments presented in the literature, the computational performance of both methods are presented and the efficiency of dynamic damping factor algorithm analyzed. We observed that, at all Reynolds numbers, our NSGS-NS solutions for both problems are in excellent agreement with the references. In particular, the SUPG/PSPG nonlinear iterations consume more linear iterations and

CPU time than the corresponding NSGS-NS solutions in the backward-facing problem. Therefore, the NSGS-NS method is computationally more efficient in this example. However, in the cavity problem, the NSGS-NS nonlinear iterative process does not converge without the damping factor process with both Reynolds numbers. In the SUPG/PSPG method, the damping algorithm significantly reduces the CPU time improving the computational performance of the method. Following the work presented here, we intend to extend the NSGS-NS method to transient problems and compressible flows given by the Navier-Stokes equations.

References

1. Armaly, B.F., Durst, F., Pereira, J., Schönung, B.: Experimental and theoretical investigation of backward-facing step flow. J. Fluid Mech. **127**, 473–496 (1983)
2. Arnold, D.N., Brezzi, F., Fortin, M.: A stable finite element for the stokes equations. Calcolo **21**(4), 337–344 (1984)
3. Baptista, R., Bento, S.S., Santos, I.P., Lima, L.M., Valli, A.M.P., Catabriga, L.: A multiscale finite element formulation for the incompressible Navier-Stokes equations. In: Gervasi, O., et al. (eds.) ICCSA 2018. LNCS, vol. 10961, pp. 253–267. Springer, Cham (2018). https://doi.org/10.1007/978-3-319-95165-2_18
4. Bazilevs, Y., Calo, V., Cottrell, J., Hughes, T., Reali, A., Scovazzi, G.: Variational multiscale residual-based turbulence modeling for large eddy simulation of incompressible flows. Comput. Methods Appl. Mech. Eng. **197**(1–4), 173–201 (2007)
5. Brenner, S.C., Scott, L.R.: The Mathematical Theory of Finite Element Methods. Texts in Applied Mathematics. Springer, New York (2002)
6. Brezzi, F.: On the existence, uniqueness and approximation of saddle-point problems arising from lagrangian multipliers. ESAIM: Math. Model. Numer. Anal. - Modélisation Mathématique et Analyse Numérique **8**(R2), 129–151 (1974)
7. Brezzi, F., Bristeau, M., Franca, L., Mallet, M., Roge, G.: A relationship between stabilized finite element methods and the Galerkin method with bubble functions. Comput. Methods Appl. Mech. Eng. **96**(1), 117–129 (1992)
8. Brooks, A.N., Hughes, T.J.R.: Streamline Upwind/Petrov-Galerkin formulations for convection dominated flows with particular emphasis on the incompressible Navier-Stokes equations. Comput. Methods Appl. Mech. Eng. **32**, 199–259 (1982)
9. Calo, V.M.: Residual-based multiscale turbulence modeling: finite volume simulations of bypass transition. Ph.D. thesis, Stanford University (2005)
10. Codina, R., Blasco, J.: A stabilized finite element method for generalized stationary incompressible flows. Comput. Methods Appl. Mech. Eng. **190**, 2681–2706 (2001)
11. Codina, R., Badia, S., Baiges, J., Principe, J.: Variational Multiscale Methods in Computational Fluid Dynamics, pp. 1–28. American Cancer Society (2017)
12. Elias, R.N., Coutinho, A.L.G.A., Martins, M.A.D.: Inexact Newton-type methods for non-linear problems arising from the SUPG/PSPG solution of steady incompressible Navier-Stokes equations. J. Braz. Soc. Mech. Sci. Eng. **26**, 330–339 (2004)
13. Erturk, E.: Numerical solutions of 2-D steady incompressible flow over a backward-facing step, part i: high reynolds number solutions. Comput. Fluids **37**(6), 633–655 (2008)
14. Erturk, E., Corke, T.C., Gökçöl, C.: Numerical solutions of 2-D steady incompressible driven cavity flow at high reynolds numbers. Int. J. Numer. Methods Fluids **48**(7), 747–774 (2005)

15. Franca, L., Farhat, C.: Unusual stabilized finite element methods and residual free bubbles. Comput. Methods Appl. Mech. Eng. **123**(1–4), 299–308 (1995)
16. de Frutos, J., John, V., Novo, J.: Projection methods for incompressible flow problems with weno finite difference schemes. J. Comput. Phys. **309**, 368–386 (2016)
17. Gartling, D.K.: A test problem for outflow boundary conditions-flow over a backward-facing step. Int. J. Numer. Methods Fluids **11**(7), 953–967 (1990)
18. Geuzaine, C., Remacle, J.F.: Gmsh: a 3-D finite element mesh generator with built-in pre- and post-processing facilities. Int. J. Numer. Methods Eng. **79**(11), 1309–1331 (2009)
19. Gravemeier, V.: The variational multiscale method for laminar and turbulent flow. Arch. Comput. Methods Eng. **13**(2), 249 (2006)
20. Hachem, E., Rivaux, B., Kloczko, T., Digonnet, H., Coupez, T.: Stabilized finite element method for incompressible flows with high reynolds number. J. Comput. Phys. **229**(23), 8643–8665 (2010)
21. Hood, P., Taylor, C.: Navier-stokes equations using mixed interpolation. In: Finite Element Methods in Flow Problems, pp. 121–132 (1974)
22. Hughes, T.J.R.: Multiscale phenomena: green's functions, the Dirichlet-to-Neumann formulation, subgrid scale models, bubbles and the origins of stabilized methods. Comput. Methods Appl. Mech. Eng. **127**(1–4), 387–401 (1995)
23. Hughes, T.J., Franca, L.P., Balestra, M.: A new finite element formulation for computational fluid dynamics. v. circumventingthe Babuska-Brezzi condition: a stable Petrov-Galerkin formulation of the Stokes problem accommodating equal-order interpolations. Comput. Methods Appl. Mech. Eng. **59**, 85–99 (1986)
24. Hughes, T., Tezduyar, T.: Finite element methods for first-order hyperbolic systems with particular emphasis on the compressible Euler equations. Comput. Methods Appl. Mech. Eng. **45**, 217–284 (1984)
25. John, V., Knobloch, P.: On spurious oscillations at layers diminishing (SOLD) methods for convection-diffusion equations: part ii-analysis for P1 and Q1 finite elements. Comput. Methods Appl. Mech. Eng. **197**(21–24), 1997–2014 (2008)
26. Lins, E.F., Elias, R.N., Guerra, G.M., Rochinha, F.A., Coutinho, A.L.G.A.: Edge-based finite element implementation of the residual-based variational multiscale method. Int. J. Numer. Methods Fluids **61**(1), 1–22 (2009)
27. Masud, A., Khurram, R.: A multiscale finite element method for the incompressible Navier-Stokes equations. Comput. Methods Appl. Mech. Eng. **195**(13–16), 1750–1777 (2006)
28. Santos, I.P., Almeida, R.C.: A nonlinear subgrid method for advection-diffusion problems. Comput. Methods Appl. Mech. Eng. **196**, 4771–4778 (2007)
29. Tezduyar, T.E.: Adaptive determination of the finite element stabilization parameters. In: Proceedings of the ECCOMAS Computational Fluid Dynamics Conference, September 2001
30. Valli, A.M., Almeida, R.C., Santos, I.P., Catabriga, L., Malta, S.M., Coutinho, A.L.: A parameter-free dynamic diffusion method for advection-diffusion-reaction problems. Comput. Math. Appl. **75**(1), 307–321 (2018)